Computational and Applied Mathematics (2025) 44:184
https://doi.org/10.1007/s40314-025-03155-5

Local Fourier analysis of multigrid methods with ILU smoother for triangular grids using aggressive coarsening

Grazielli Vassoler-Rutz[1] · Michely L. Oliveira[2] · Marcio A. V. Pinto[3]

Received: 16 May 2023 / Revised: 15 February 2025 / Accepted: 19 February 2025

Abstract
This work investigates multigrid methods on triangular grids with aggressive coarsening and incomplete factorization smoothers. Two-grid local Fourier analysis is employed to optimize smoothing parameters and ensure rapid convergence under aggressive coarsening. A two-dimensional diffusion problem serves as a test case, demonstrating that aggressive coarsening is a viable alternative to standard coarsening. The results highlight substantial computational and memory savings, making aggressive coarsening an efficient choice for multigrid method.

Keywords Local Fourier analysis · Diffusion problem · Asymptotic convergence factor · Computational work · Smoothing analysis

Mathematics Subject Classification 65N55 · 65B99 · 65F10

1 Introduction

The numerical solution of partial differential equations (PDEs) often involves solving large, sparse algebraic systems, a task of great interest due to its broad range of applications. The multigrid method was developed to efficiently solve these systems by combining grid smoothing at the finest levels with a coarsening strategy. However, in multi-core parallel

Michely L. Oliveira and Marcio A. V. Pinto have contributed equally to this work.

✉ Grazielli Vassoler-Rutz
grazielli.vassoler@ifsc.edu.br

Michely L. Oliveira
michely-lais@hotmail.com

Marcio A. V. Pinto
marcio_villela@ufpr.br

1 Department of Mathematics, Federal Institute of Education, Science and Technology of Santa Catarina (IFSC), Chapecó, Santa Catarina 89802155, Brazil

2 Department of Mathematics, Graduate Program in Numerical Methods in Engineering, Federal University of Paraná (UFPR), St. Evaristo F. Ferreira da Costa, Curitiba, Paraná 1531980, Brazil

3 Department of Mechanical Engineering, Federal University of Paraná (UFPR), Ave. Cel. Francisco H. dos Santos, Curitiba, Paraná 1531980, Brazil

Published online: 13 March 2025

architectures, visiting coarser levels can lead to performance losses in the multigrid method (Brannick et al. 2015).

Several researchers have explored aggressive coarsening combined with various multigrid parameters, such as smoother and grid structures, to analyze and improve the performance of the standard algorithm. Local Fourier Analysis (LFA) has been widely employed in these studies. Results using point-wise smoothers and quadrangular grids can be found in Wienands and Joppich (2005) and Zubair et al. (2007), while studies involving triangular grids are presented in Gaspar et al. (2009). Aggressive coarsening with polynomial smoothers was investigated by Brannick et al. (2015). These studies observed that the total number of floating-point operations tends to increase with aggressive coarsening compared to standard coarsening because point-wise smoother are insufficient for reducing a large subspace of the high-frequency error components.

Incomplete factorization methods (ILU), which approximate the exact LU factorization of a matrix A, are highly robust and can, in principle, be applied to any sparse matrix (Pinto et al. 2016).

Choosing an appropriate smoother is essential for ensuring optimal multigrid performance. ILU methods, which were first introduced in Buleev (1960) and Oliphant (1961, 1962), are widely used for this purpose. Johannsen (2005) solved an anisotropic diffusion problem by discretizing the equations using the Finite Element Method (FEM) and employing the ILU 9-point method to solve the resulting linear systems. ILU methods have also been described as a matrix division technique in Varga (1960, 1962). For further details, refer to Hackbusch (1994) and Axelsson (1994).

The importance of parameter selection in multigrid methods is emphasized in foundational works such as Hackbusch (1985), Stüben and Trottenberg (1982), Trottenberg et al. (2001) and Wesseling (1992). These studies demonstrate that parameter choices are critical to ensuring convergence and that even small adjustments can significantly impact performance. The ILU method, initially introduced as a smoother by Wesseling (1982) and Wesseling and Sonneveld (1980), has since been widely applied in diverse areas (Johannsen 2005; Stevenson 1994; Wittum 1989a, b), including problems involving anisotropy (Khalil 1989; Oertel and Stüben 1989; Stevenson 1994; Wittum 1989b).

In Pinto et al. (2016), the robustness of the ILU smoother for solving various two-dimensional diffusion problems on triangular grids, including different types of anisotropy, was demonstrated. The study achieved excellent results for oblique flow problems and semi-structured grids.

Accurate solutions can also be attained by combining multigrid methods with repeated Richardson extrapolation (Silva et al. 2021). LFA plays a crucial role in these parameter choice, as it predicts multigrid performance by estimating convergence rates through parameter variation. LFA assumes that boundary conditions are neglected by formally defining the discrete operator, requiring a constant stencil on an infinite regular grid. However, this assumption does not hold for ILU techniques (Pinto et al. 2016).

Wienands and Joppich (2005) conducted a comprehensive study of LFA and its applications to various problems, including anisotropic diffusion equations. Their work calculated the convergence factors of the multigrid method, accounting for variations in smoothers, restriction operators, and extension operators. Johannsen (2005) employed LFA to emphasize the distinctive smoothing properties of the ILU method. Additionally, the smoothing behavior of ILU-type smoothers on triangular and rectangular grids, as well as detailed analyses of multigrid convergence using two- and three-grid approaches, have been extensively studied in works such as Chan (1991), Johannsen (2005), Wittum (1989a, b) and Pinto et al. (2016).

LFA has also been explored for anisotropic problems, with studies by Oliveira et al. (2018) and Rutz et al. (2019) demonstrating the effectiveness of multigrid methods in these cases. These works evaluated different multigrid parameters, such as restriction and prolongation operators, along with smoother like ILU (Rutz et al. 2019) and xy-zebra Gauss–Seidel (Oliveira et al. 2018). Both studies reported strong performance, particularly for problems with high anisotropy.

In this work, we aim to provide a flexible framework for investigating these methods under aggressive coarsening conditions. Unlike previous studies (Gaspar et al. 2009; Brannick et al. 2015; Pinto et al. 2016; Wittum 1989b; Rutz et al. 2019), the novelty of this paper lies in applying Local Fourier Analysis on triangular grids while using aggressive coarsening and ILU as a smoother. Our findings reveal that aggressive coarsening is as robust and efficient as standard coarsening.

This paper is organized as follows: in Sect. 2, the ILU techniques applied to triangular grids are introduced. Section 3 explains how LFA is performed for multigrid methods with ILU smoothers, detailing the smoothing process and two-grid LFA for aggressive coarsening. Section 4 presents results for the two-dimensional Poisson equation, while Sect. 5 discusses the computational cost and includes a complexity analysis to confirm the methodology is efficiency. Finally, Sect. 6 provides the conclusions and final remarks.

2 ILU decomposition techniques for structured triangular grids

Systems of equations involving large and sparse matrices often result from the discretization of partial differential equations (PDEs). In the specific problem under study, these matrices are also symmetric. This section introduces the ILU decomposition for such matrices, using a triangular grid for discretization with standard coarsening. To construct a triangular grid, the midpoints of the edges of a regular triangle are connected, dividing it into four congruent triangles. Section 3 will provide details on aggressive coarsening, smoothing, and two-grid analysis. Referring to the triangular grid depicted in Fig. 1, the ILU decomposition is defined as follows:

$$G_\ell = \{\mathbf{x} = (x, y)|_{\{\mathbf{e}_1,\mathbf{e}_2\}} \mid x = k_x\, h_x,\ \ y = k_y\, h_y,\ \ k_x = 0, \ldots, 2^\ell,\ k_y = 0, \ldots, k_x\}. \quad (1)$$

Based on the geometry of the triangular grid shown in Fig. 1, we define a new unit vector basis $\mathbf{e}_1$ and $\mathbf{e}_2$ for this grid. Here, h_x represents the grid spacing in the x-direction, and h_y represents the spacing in the y-direction. A fixed number, ℓ, of refinement steps is also considered. The coordinates $(x, y)|_{\{\mathbf{e}_1,\mathbf{e}_2\}}$ refer to the position in the new coordinate system, while the indexing system (k_x, k_y) provides a double-index local numbering to label neighboring nodes and define the stencil of the sparse matrix.

For the specific case of this study, the ILU 7-point decomposition (see Fig. 1) is efficient (Johannsen 2005; Wittum 1989a, b). The stencil form of the symmetric matrix A is given by

$$A^{ij} = \begin{bmatrix} \cdot & a_{i,j+1} & a_{i+1,j+1} \\ a_{i-1,j} & a_{i,j} & a_{i+1,j} \\ a_{i-1,j-1} & a_{i,j-1} & \cdot \end{bmatrix}. \quad (2)$$

Considering $A = M - R$, the incomplete LU decomposition (ILU) is obtained if the matrix M is replaced by

$$M = LD^{-1}U,$$

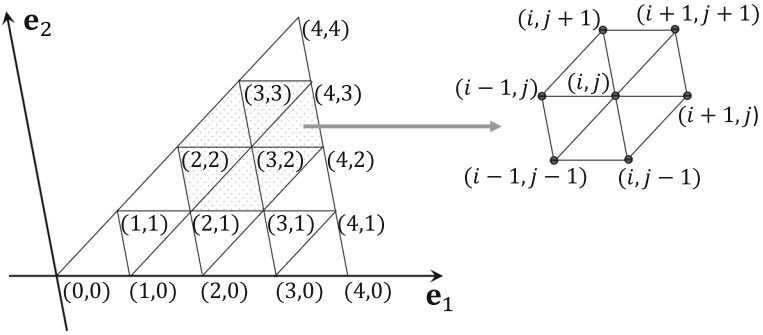

Fig. 1 New basis in $\mathbb{R}^2$ aligned with the geometry of the triangular grid, showing the local numbering of the regular grid after two refinement levels and the numbering for the stencil operator (adapted from Pinto et al. (2016))

where R is the residual matrix, D is a diagonal matrix, L and U maintain the same sparsity as matrix A. A better way to write the matrix M, considering only the matrices L and D, is given by

$$M = (L + D)D^{-1}(L^T + D).$$

Based on this system, where the iteration matrix is defined as $(I - M^{-1}A) = (I - (L^T + D)^{-1}D(L + D)^{-1}A)$, the iterative process is formulated as follows:

$$(L + D)D^{-1}(L^T + D)u^{m+1} = f + Ru^m. \tag{3}$$

In this work, we focus on the specific case of the 7-point ILU decomposition, which will be introduced and utilized in the subsequent sections along with a lexicographic ordering scheme proceeding west-to-east and south-to-north. Based on the node numbering provided in Fig. 1, the iterative process described by Eq. (3) can be expressed in its stencil form as:

$$L^{ij} = \begin{bmatrix} \cdot & \cdot & \cdot \\ l_{i-1,j} & \cdot & \cdot \\ l_{i-1,j-1} & l_{i,j-1} & \cdot \end{bmatrix}, \quad D^{ij} = \begin{bmatrix} \cdot & \cdot & \cdot \\ \cdot & d_{i,j} & \cdot \\ \cdot & \cdot & \cdot \end{bmatrix},$$
$$R^{ij} = \begin{bmatrix} r_{i-1,j+1} & \cdot & \cdot \\ \cdot & \cdot & \cdot \\ \cdot & \cdot & r_{i+1,j-1} \end{bmatrix}. \tag{4}$$

In ILU decomposition, certain elements are discarded during the elimination process. Techniques have been developed to mitigate this effect by compensating for the discarded elements. One such technique involves adding the absolute values of the discarded elements to the main diagonal of U. This approach, known as *modified incomplete factorization* (MILU), will hereafter be referred to as ILU$_\sigma$. Using Eq. (3), the 7-point ILU decomposition can be expressed in its recursive form for a symmetric matrix A as follows:

$$A = (L + D_\sigma)D_\sigma^{-1}(L^T + D_\sigma) - R_\sigma,$$

with $D_\sigma = D + \sigma\widetilde{D}$, where the diagonal matrix $\widetilde{D}$ has diagonal elements of the form $\widetilde{d}_{ii} = \sum_{j \neq i} |r_{ij}^\sigma|$, we consider ILU$_\sigma$ and $R_\sigma = (r_{ij}^\sigma)$ analogous to $R = (r_{ij})$.

To simplify the notation, we modify the iteration matrices A and R. This simplified expression will be utilized in the subsequent sections, primarily for the calculation of Fourier symbols. Therefore, we consider:

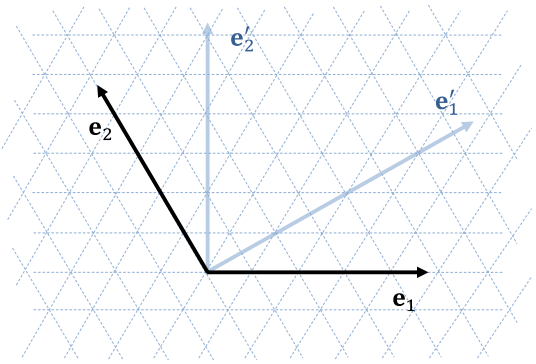

Fig. 2 Non-orthogonal basis $\{\mathbf{e}_1, \mathbf{e}_2\}$ in $\mathbb{R}^2$, and its dual basis $\{\mathbf{e}_1', \mathbf{e}_2'\}$ (Pinto et al. 2016)

$$(I - M^{-1}A) = (I - (A + R)^{-1}A) = (A + R)^{-1}R. \tag{5}$$

Remark 1 Equation (5) will be used later to derive the smoothing factor.

3 One- and two-grid LFA for multigrid using ILU as smoothers

Local Fourier Analysis (LFA) is a powerful tool for the quantitative analysis and design of efficient multigrid methods. This section introduces the general concepts and terminology of LFA. To apply LFA, certain simplifications are made: an infinite grid is assumed, and boundary conditions are ignored.

3.1 Notation and basics of LFA for ILU smoothers

To apply LFA, the matrix A must have a constant stencil, a property not inherently satisfied by L, U, and R. However, the decomposition of A approximates a constant stencil near the boundaries. The works of Gaspar et al. (2009) and Rodrigo et al. (2012) provide a detailed and comprehensive formulation for applying LFA to triangular grids and are considered here. Additionally, a new coordinate system in the frequency space is introduced, utilizing a non-orthogonal unit basis $\mathbb{R}^2$ $\{\mathbf{e}_1, \mathbf{e}_2\}$.. This non-orthogonal basis is defined by $\{\mathbf{e}_1', \mathbf{e}_2'\}$, derived from the geometry of the grid shown in Fig. 2. The basis vectors satisfy the condition $(\mathbf{e}_i', \mathbf{e}_j') = \delta_{ij}$, $1 \leq i, j \leq 2$.

In the context of LFA, we consider grid functions where $\mathbf{x}$ varies over the infinite grid, allowing the influence of boundaries to be neglected. Additionally, θ is introduced as a continuous parameter that represents the frequency of the grid function. Hence, the grid functions can be expressed

$$\varphi_h(\boldsymbol{\theta}, \mathbf{x}) = e^{\imath \boldsymbol{\theta} \cdot \mathbf{x}} = e^{\imath \theta_1 x_1} e^{\imath \theta_2 x_2}, \quad \boldsymbol{\theta} \in \Theta_h = (-\pi, \pi] \times (-\pi, \pi].$$

According to Wesseling (1992), the formulation of LFA for ILU-type smoothers on an infinite grid assumes that the stencils in Eqs. (4) are no longer dependent on (i, j). Therefore, the coefficients of these stencils are calculated considering:

$$\begin{bmatrix} \cdot & a_{0,-1} & a_{-1,-1} \\ a_{-1,0} & a_{0,0} & a_{-1,0} \\ a_{-1,-1} & a_{0,-1} & \cdot \end{bmatrix} = \begin{bmatrix} \cdot & \cdot & \cdot \\ l_{-1,0} & d_{0,0} & \cdot \\ l_{-1,-1} & l_{0,-1} & \cdot \end{bmatrix} \begin{bmatrix} \cdot & \cdot & \cdot \\ \cdot & d_{0,0}^{-1} & \cdot \\ \cdot & \cdot & \cdot \end{bmatrix} \begin{bmatrix} \cdot & l_{0,-1} & l_{-1,-1} \\ \cdot & d_{0,0} & l_{-1,0} \\ \cdot & \cdot & \cdot \end{bmatrix} - \begin{bmatrix} r_{1,-1} & \cdot & \cdot \\ \cdot & 2\sigma|r_{1,-1}| & \cdot \\ \cdot & \cdot & r_{1,-1} \end{bmatrix}. \tag{6}$$

Thus, we obtain a system of non-linear equations. Given that $a_{0,-1} = a_{-1,0}$, it follows that $l_{0,-1} = l_{-1,0}$, and $l_{-1,-1} = a_{-1,-1}$. This system can be efficiently computed (Pinto et al. 2016) using the following recursive process:

$$\begin{aligned} &d_{0,0}^0 = a_{0,0},\ l_{-1,0}^0 = a_{-1,0},\ l_{0,-1}^0 = a_{0,-1},\ r_{1,-1}^0 = \frac{l_{-1,0}^0}{d_{0,0}^0} l_{0,-1}^0 \\ &\text{For } k = 1, \ldots \\ &l_{0,-1}^k = a_{0,-1} - \frac{l_{-1,-1}}{d_{0,0}^{k-1}} l_{-1,0}^{k-1}, \\ &l_{-1,0}^k = a_{-1,0} - \frac{l_{-1,-1}}{d_{0,0}^{k-1}} l_{0,-1}^k, \\ &d_{0,0}^k = \frac{-1}{d_{0,0}^{k-1}} \left(l_{-1,-1}^2 + (l_{-1,0}^k)^2 + (l_{0,-1}^k)^2 \right) + a_{0,0} + 2\sigma |r_{1,-1}^{k-1}|, \\ &r_{1,-1}^k = \frac{l_{-1,0}^k}{d_{0,0}^k} l_{0,-1}^k. \end{aligned} \tag{7}$$

By solving the recursive process given in Eq. (7), we obtain the ILU_σ decomposition and the iteration matrix can be expressed as shown in Eq. (5).

3.2 Smoothing analysis

For the smoothing analysis, the eigenvalues (Fourier symbols) of the matrix ILU_σ are calculated as follows

$$\widetilde{S}(\boldsymbol{\theta}) = \frac{\widetilde{R}(\boldsymbol{\theta})}{\widetilde{A}(\boldsymbol{\theta}) + \widetilde{R}(\boldsymbol{\theta})}. \tag{8}$$

Considering the stencil notation presented in Eq. (6), we have

$$\widetilde{A}(\boldsymbol{\theta}) = a_{0,-1}e^{-\iota\theta_2} + a_{-1,-1}e^{\iota(\theta_1-\theta_2)} + a_{-1,0}e^{-\iota\theta_1} + a_{0,0} + a_{-1,0}e^{\iota\theta_1} + a_{-1,-1}e^{-\iota(\theta_1-\theta_2)} + a_{0,-1}e^{\iota\theta_2},$$

and

$$\widetilde{R}(\boldsymbol{\theta}) = p_1 e^{\iota(2\theta_1-\theta_2)} + p_3 + p_2 e^{\iota(-2\theta_1+\theta_2)},$$

with $p_1 = l_{0,-1}d_{0,0}^{-1}l_{-1,0}$, $p_2 = l_{-1,0}d_{0,0}^{-1}l_{0,-1}$, $p_3 = \sigma|p_1 + p_2|$

Remark 2 In Eq. (8) the expression $\widetilde{A}(\boldsymbol{\theta}) + \widetilde{R}(\boldsymbol{\theta})$ originates from the stencils of the matrices A and R, respectively. Therefore, it will not be necessary to approach the inversion of $A + R$ given by Eq. (5).

The method converges to values of $|\widetilde{S}(\boldsymbol{\theta})| < 1$ with $\boldsymbol{\theta} \in \Theta_h$. The process outlined above, which produces ILU_σ, will be used as a multigrid smoother. Thus, we need to analyze the smoothing properties of ILU, specifically how this smoother reduces the high-frequency

components of the error. Since certain Fourier modes are not resolved on the coarse grid, the classification of "high" and "low" frequencies is done based on the grid in question.

Then, LFA is performed considering aggressive coarsening. In this case, the coarse grid is denoted by $\Omega_{2^k h}$, with $k \geq 1$, where k is an integer. For $k = 1$, we obtain the well-known standard coarsening. The high and low frequencies on this grid are given by

all frequencies: $\Theta_h = (-\pi/h_1, \pi/h_1] \times (-\pi/h_2, \pi/h_2]$,

low frequencies: $\Theta_{2^k h} = (-\pi/(2^k h_1), \pi/(2^k h_1)] \times (-\pi/(2^k h_2), \pi/(2^k h_2)]$,

high frequencies: $\Theta_h \setminus \Theta_{2^k h}$.

Fourier modes are the eigenvalues of the smoothing operator S_h, so the smoothing factor can be calculated as:

$$\mu = \sup_{\boldsymbol{\theta} \in \Theta_h \setminus \Theta_{2^k h}} |\widetilde{S}(\boldsymbol{\theta})|. \tag{9}$$

3.3 Two-grid LFA for aggressive coarsening

In addition to analyzing the smoother performance (smoothing analysis), LFA allows for predicting multigrid behavior through a two-grid analysis. In this case, besides the smoother, the transfer operators between grids (restriction and prolongation) are also considered. This section presents a two-grid LFA that accounts for aggressive coarsening, transitioning from a fine step size h to a coarse step size $2^k h$.

For $k = 1$, we have $2h$-coarsening, which corresponds to first-level coarsening (standard coarsening). For $k = 2$, we have $4h$-coarsening, which corresponds to second-level coarsening. For $k = 3$, we have $8h$-coarsening, corresponding to third-level coarsening, and so on.

Therefore, the error propagation operator ($e_h^{m+1} = M_h^{2^k h} e_h^m$) in the two-grid method must be considered, and it is given by:

$$M_h^{2^k h} = S_h^{\nu_2} (I_h - I_{2^k h}^h A_{2^k h}^{-1} I_h^{2^k h} A_h) S_h^{\nu_1},$$

where S_h is the smoothing process, and ν_1 and ν_2 represent the pre- and post-smoothing steps, respectively. A_h and $A_{2^k h}$ are discrete operators on the fine and coarse grids, respectively, where $A_{2^k h}$ is a known coarse-grid correction operator. The restriction operator $I_h^{2^k h}$ and the prolongation operator $I_{2^k h}^h$ are the transfer operators. Consider h and $2^k h$ as two consecutive fine and coarse grids, where $2^k h$ results from applying k-level aggressive coarsening. The asymptotic convergence factor ρ, obtained from the two-grid analysis, is the spectral radius of the operator $M_h^{2^k h}$.

By denoting the fine-grid as Ω_h and the coarse-grid as $\Omega_{2^k h}$, it is necessary to perform the Fourier analysis. For any integer $k \geq 1$, the low frequencies $\Theta_{2^k h} = (-\pi/(2^k h), \pi/(2^k h)] \times (-\pi/(2^k h), \pi/(2^k h)]$ are associated with $4^k - 1$ high frequencies through the coarse-grid correction operator. In this case, the Fourier space can be subdivided into 4^k-dimensional subspaces $\mathcal{F}^{2^k h}(\boldsymbol{\theta})$, which are obtained by the Fourier modes corresponding to the frequencies 4^k, so

$$\mathcal{F}(\Omega_h) = \bigoplus_{\Theta_{2^k h}} \mathcal{F}^{2^k h}(\boldsymbol{\theta}).$$

A representation of the two-grid operator in Fourier space can be expressed as a block matrix, which simplifies the calculation of the spectral radius of the iteration matrix. In this case, the spectral radius is determined by calculating the maximum value of the block matrix spectrum.

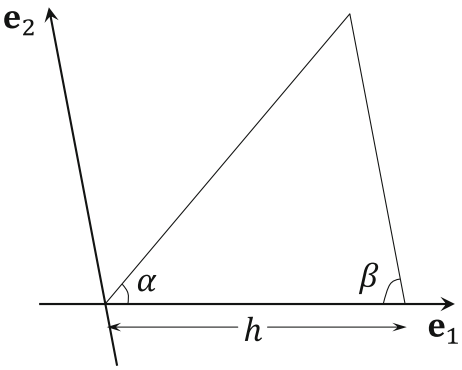

Fig. 3 Triangular domain characterized by the angles α and β, as well as the length h (Pinto et al. 2016)

For this reason, $M_h^{2^k h}$ is represented as a block-diagonal matrix composed of $(4^k \times 4^k)$–blocks, denoted

$$\widetilde{M}_h^{2^k h}(\boldsymbol{\theta}) = \widetilde{S}_h^{\nu_2}(\boldsymbol{\theta})\widetilde{C}_h^{2^k h}(\boldsymbol{\theta})\widetilde{S}_h^{\nu_1}(\boldsymbol{\theta}).$$

Considering the subspaces $\mathcal{F}^{2^k h}(\boldsymbol{\theta})$, $\widetilde{S}_h(\boldsymbol{\theta})$ represents the block-matrix form of the smoother. Similarly, the block-matrix $\widetilde{C}_h^{2^k h}(\boldsymbol{\theta})$ denotes the representation of the coarse-grid correction operator, which is derived from the Fourier representation as

$$\widetilde{C}_h^{2^k h} = \widetilde{I}_h - \widetilde{I}_{2^k h}^{h} \widetilde{A}_{2^k h}^{-1} \widetilde{I}_h^{2^k h} \widetilde{A}_h.$$

In this way, the spectral radius $\rho(M_h^{2^k h})$, which represents the asymptotic two-grid convergence factor, can be determined by calculating the spectral radius of these smaller matrices

$$\rho_{2g} = \rho(M_h^{2^k h}) = \sup_{\boldsymbol{\theta} \in \Theta_{2^k h}} \rho(\widetilde{M}_h^{2^k h}(\boldsymbol{\theta})). \tag{10}$$

The following section presents the results of the LFA using the ILU smoother, with both aggressive and standard coarsening, applied to a specific problem.

4 Local Fourier analysis results

The mathematical model used for applying the LFA is the two-dimensional diffusion equation, expressed as

$$\nabla \cdot (K \nabla u(\mathbf{x})) = f(\mathbf{x}), \ \mathbf{x} \in \Omega, \tag{11}$$

where $K = [k_{ij}]_{2\times 2}$ is referred to as the diffusion tensor (Pinto et al. 2016) and possesses the properties of symmetry and positive definiteness. In this section, Ω represents a triangular domain. Figure 3 illustrates a triangular domain defined by angles α and β, as well as a side length h.

The problem in (11) can be discretized using the Finite Element Method (FEM) with a triangular grid and multiple levels of refinement in the domain Ω. The stencil resulting from this discretization is given by Pinto et al. (2016).

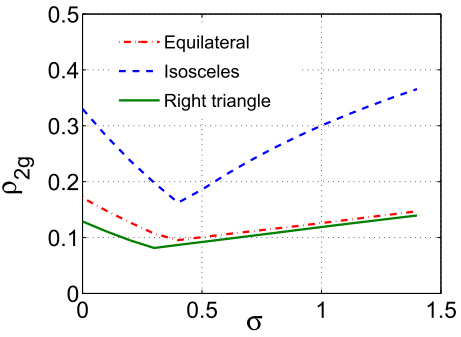

Fig. 4 Two-grid convergence factors predicted by the LFA (ρ_{2g}) as a function of various values of σ for three representative triangular domains. The results are shown for $\nu = 1$ and $2h$-coarsening (see Pinto et al. (2016))

$$A_h = \frac{k_{11}}{h^2}\begin{bmatrix} 0 & 0 & 0 \\ -1 & 2 & -1 \\ 0 & 0 & 0 \end{bmatrix} + \frac{k_{12}}{h^2}\begin{bmatrix} 0 & ca+cb & -ca-cb \\ ca-cb & -2(ca-cb) & ca-cb \\ -ca-cb & ca+cb & 0 \end{bmatrix} + \frac{k_{22}}{h^2}\begin{bmatrix} 0 & -ca^2-ca\,cb & -cb^2-ca\,cb \\ ca\,cb & 2(ca^2+cb^2+ca\,cb) & ca\,cb \\ -cb^2-ca\,cb & -ca^2-ca\,cb & 0 \end{bmatrix}, \tag{12}$$

where $ca = \cot(\alpha)$ and $cb = \cot(\beta)$.

In numerous applications, the direction of anisotropy is not readily apparent. Consequently, the selection of an appropriate smoother is essential. The ILU smoother, due to its exceptional robustness, is an excellent option in such scenarios. Pinto et al. (2016) presented results for the ILU smoother with standard coarsening.

The subsequent section will present the results from the LFA that utilized the ILU smoother for the Laplace equation ($K = I$) with aggressive coarsening. Three specific coarsening strategies $2h$, $4h$, and $8h$ will be analyzed. The remaining multigrid parameters are assumed to follow standard configurations. More precisely, canonical interpolation, restriction for linear finite elements, and direct discretization on the coarse grids will be considered (Trottenberg et al. 2001; Wesseling 1992).

4.1 The 2 h-coarsening (standard coarsening)

The Local Fourier Analysis (LFA) results for $2h$-coarsening on triangular domains using the ILU_σ smoother will be presented initially. Three representative triangular domains are considered: an equilateral triangle (with angles $\alpha = \beta = 60°$), an isosceles right triangle (characterized by angles $\alpha = \beta = 45°$), and an isosceles triangle with a very small angle (with characterized by $\alpha = \beta = 80°$).

Since it is difficult to derive an analytical expression for the optimal value of the σ-parameter (σ_{opt}), we resort to numerically derived values. Specifically, the two-grid convergence factors (ρ_{2g}) associated with ILU_σ, predicted by LFA, are shown in Fig. 4 for $\nu = \nu_1 + \nu_2 = 1$ (where ν_1 and ν_2 are the numbers of pre- and post-smoothing steps, respectively) and $\sigma \in [0, 1.4]$. The figure illustrates the optimal value of this parameter. Notably, the optimal value of σ is approximately $\sigma_{opt}(Equilateral) \approx \sigma_{opt}(Isosceles) \approx \sigma_{opt}(Right) \approx 0.5$ as recommended by Wesseling (1992) and Wittum (1989b).

Table 1 presents both the two-grid convergence factors as predicted by the Local Fourier Analysis (ρ_{2g}) and the experimentally computed asymptotic convergence factor (ρ_h) utilizing the $\text{ILU}_{0.5}$ smoother with an F-cycle. The fine grid is generated after 10-refinement levels.

Table 1 Two-grid convergence factors predicted by the LFA (ρ_{2g}) alongside the experimentally computed asymptotic convergence factor (ρ_h) using $\text{ILU}_{0.5}$ for three representative triangular domains, varying numbers of smoothing steps (ν), and $2h$-coarsening

ν	Equilateral		Right		Isosceles	
	ρ_{2g}	ρ_h	ρ_{2g}	ρ_h	ρ_{2g}	ρ_h
1	0.101	0.101	0.092	0.091	0.187	0.187
2	0.028	0.027	0.036	0.035	0.075	0.074
3	0.015	0.015	0.023	0.023	0.044	0.044
4	0.011	0.010	0.017	0.017	0.033	0.033

Table 2 Two-grid convergence factors predicted by LFA, using the $\text{ILU}_{0.5}$ smoother with $\nu = 2$ for different triangles in function of two of their angles and $2h$-coarsening

α/β	10	20	30	40	50	60	70	80	90
10	0.095	0.091	0.087	0.087	0.084	0.083	0.081	0.081	0.114
20	0.082	0.076	0.072	0.063	0.065	0.062	0.061	0.075	0.114
30	0.067	0.062	0.057	0.053	0.050	0.047	0.047	0.074	0.113
40	0.054	0.049	0.045	0.042	0.039	0.036	0.046	0.073	0.113
50	0.043	0.039	0.036	0.033	0.031	0.028	0.046	0.073	0.113
60	0.035	0.032	0.029	0.027	0.025	0.028	0.046	0.073	0.113
70	0.029	0.026	0.025	0.023	0.025	0.028	0.046	0.074	0.114
80	0.024	0.023	0.025	0.027	0.031	0.036	0.047	0.075	0.114
90	0.024	0.026	0.029	0.033	0.039	0.047	0.061	0.081	–

These results are shown for various numbers of smoothing steps $\nu = \nu_1 + \nu_2$. Notably, there is strong agreement between ρ_{2g} and ρ_h.

Table 1 demonstrates that the LFA predicts the asymptotic convergence factors with high accuracy, which closely match the experimentally computed values. Notably, excellent convergence rates, below 0.1, are achieved with only two smoothing steps, leading to the adoption of $\nu = 2$ for subsequent experiments. Furthermore, utilizing $\text{ILU}_{0.5}$ as the smoother within the multigrid process guarantees robust performance across various triangulations. This observation is supported by Table 2, which presents LFA-predicted two-grid convergence factors for a wide range of triangular domains, each defined by two of their angles, α and β, as depicted in Fig. 3.

Noticeably, the $\text{ILU}_{0.5}$ smoother with west-to-east and south-to-north lexicographic ordering yields satisfactory results for all the triangles analyzed, in contrast to the behavior observed with line-smoothers, such as those studied in Rodrigo et al. (2012).

Although $\sigma = 0.5$ is used for the ILU_σ smoother throughout this section due to its robustness for the problem at hand, it is important to note that for a specific problem, the value of $\sigma = 0.5$ is not necessarily the optimal one, as other values could potentially yield better results. Nevertheless, it is evident that LFA can assist in identifying the optimal value of σ.

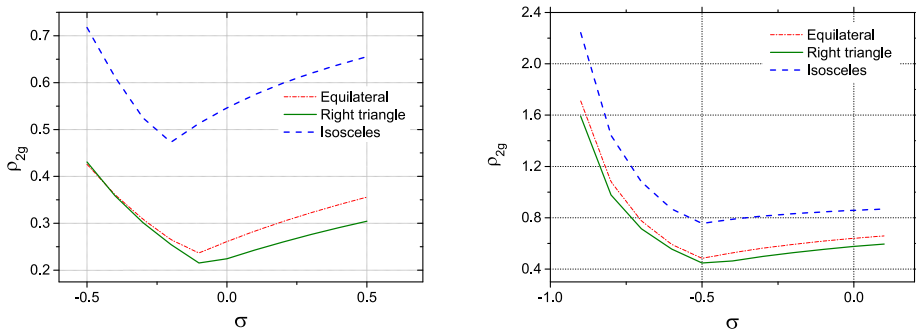

Fig. 5 Two-grid convergence factors predicted by LFA (ρ_{2g}) versus various values of σ for three representative triangular domains, $\nu = 1$, **a** σ for $4h$-coarsening and **b** σ for $8h$-coarsening

Table 3 Two-grid convergence factors predicted by LFA (ρ_{2g}) alongside the experimentally computed asymptotic convergence factor (ρ_h) using $\text{ILU}_{-0.1}$ for three representative triangular domains, different numbers of smoothing steps ν and $4h$-coarsening

ν	Equilateral		Right		Isosceles	
	ρ_{2g}	ρ_h	ρ_{2g}	ρ_h	ρ_{2g}	ρ_h
1	0.237	0.239	0.215	0.215	0.513	0.513
2	0.096	0.096	0.110	0.109	0.263	0.263
3	0.048	0.047	0.072	0.071	0.136	0.136
4	0.035	0.034	0.055	0.055	0.103	0.102

4.2 The 4 h- and 8 h-coarsening (aggressive coarsening)

This section presents the LFA results for aggressive coarsening, specifically $4h$- and $8h$-coarsening, applied to triangular domains using the ILU_σ smoother. We use the same three representative triangular domains as in Sect. 4.1. Additionally, we maintain the numerically derived values for the optimal σ (σ_{opt}). The two-grid convergence factors (ρ_{2g}) associated with ILU_σ, as predicted by the LFA, are shown in Fig. 5. These results are for $\nu = \nu_1 + \nu_2 = 1$, illustrating the optimal value of the σ parameter (σ_{opt}) for both $4h$-coarsening with $\sigma \in [-0.5, 0.5]$ and $8h$-coarsening with $\sigma \in [-0.9, 0.1]$. Note that for $4h$-coarsening (Fig. 5a), $\sigma_{opt}(Equilateral) \approx \sigma_{opt}(Isosceles) \approx \sigma_{opt}(Right) \approx -0.1$, and for $8h$-coarsening (Fig. 5b), $\sigma_{opt}(Equilateral) = \sigma_{opt}(Isosceles) = \sigma_{opt}(Right) = -0.5$.

In Table 3, for the three triangular domains with $4h$-coarsening, we present the two-grid convergence factors (ρ_{2g}) alongside the experimentally computed asymptotic convergence factor (ρ_h) when using the $\text{ILU}_{-0.1}$ smoother. These results are obtained with an F-cycle and a fine grid after 10-refinement levels. Similarly, Table 4 shows the results for $8h$-coarsening using the $\text{ILU}_{-0.5}$ smoother. Both tables include results for various numbers of smoothing steps ($\nu = \nu_1 + \nu_2$), where the symbol * denotes slow convergence (i.e., requiring up to 1000 iterations). We note that there is strong agreement between ρ_{2g} and ρ_h in both cases.

From the data in Tables 3 and 4, we can conclude that the LFA provides accurate predictions of the experimentally computed asymptotic convergence factors. In Table 3, satisfactory convergence rates close to 0.1 are achieved with four smoothing steps. Based on this, we

Table 4 Two-grid convergence factors predicted by LFA (ρ_{2g}) along with the experimentally computed asymptotic convergence factor (ρ_h) using ILU$_{-0.5}$ smoother for three representative triangular domains, different numbers of smoothing steps ν and $8h$-coarsening

ν	Equilateral		Right		Isosceles	
	ρ_{2g}	ρ_h	ρ_{2g}	ρ_h	ρ_{2g}	ρ_h
1	0.484	0.483	0.448	0.447	0.756	0.756*
2	0.269	0.269	0.246	0.245	0.572	0.571*
3	0.118	0.119	0.164	0.162	0.433	0.432*
4	0.093	0.093	0.132	0.130	0.327	0.327
5	0.067	0.067	0.107	0.106	0.247	0.247
6	0.056	0.056	0.092	0.090	0.189	0.190

Table 5 Two-grid convergence factors predicted by LFA, using the ILU$_{-0.1}$ smoother with $\nu = 4$ for different triangular domains as a function of two of their angles, and $4h$-coarsening

α/β	10	20	30	40	50	60	70	80	90
10	0.173	0.163	0.154	0.145	0.137	0.132	0.127	0.132	0.345
20	0.142	0.131	0.120	0.112	0.105	0.099	0.095	0.103	0.156
30	0.113	0.103	0.094	0.086	0.080	0.075	0.072	0.096	0.148
40	0.088	0.080	0.073	0.066	0.061	0.056	0.059	0.094	0.146
50	0.069	0.062	0.056	0.051	0.046	0.042	0.058	0.093	0.146
60	0.054	0.048	0.043	0.039	0.035	0.035	0.058	0.094	0.148
70	0.042	0.038	0.034	0.031	0.035	0.042	0.059	0.096	0.156
80	0.033	0.031	0.034	0.039	0.046	0.056	0.072	0.103	0.345
90	0.033	0.038	0.043	0.051	0.061	0.075	0.095	0.132	–

set $\nu = 4$ for the remaining experiments in this section for $4h$-coarsening. Additionally, it appears that using the ILU$_{-0.1}$ smoother in the multigrid process results in a robust algorithm that works well across different triangulations.

This observation is further supported by the results in Table 5, where the two-grid convergence factors predicted by the LFA are presented for a wide range of triangular domains characterized by two of their angles, α and β.

In Table 4, satisfactory convergence rates near 0.1 and below 0.2 are achieved with $\nu = 6$ for $8h$-coarsening. As observed in the previous cases, the ILU$_{-0.5}$ smoother results in a robust algorithm that works well for various triangulations. This is further confirmed in Table 6, where the two-grid convergence factors predicted by LFA are presented for a wide range of triangular domains.

It is also noted that the 7-point ILU smoother for both $4h$- and $8h$-coarsening leads to satisfactory convergence factors when the recommended σ and ν, values are used, especially when the lines are processed in the west-to-east and south-to-north lexicographic order. For another satisfactory combination of lexicographic ordering directions, refer to Pinto et al. (2016).

Although $\sigma = -0.1$ (for $4h$-coarsening) and $\sigma = -0.5$ (for $8h$-coarsening) are used throughout this section due to their robustness for the problem at hand, it is important to note that these values are not necessarily optimal for every concrete problem. There may be other

Table 6 Two-grid convergence factors predicted by LFA, using the $\text{ILU}_{-0.5}$ smoother with $\nu = 6$ for various triangles as a function of two of their angles and $8h$-coarsening

α/β	10	20	30	40	50	60	70	80	90
10	0.285	0.267	0.251	0.235	0.219	0.204	0.205	1.179	19.426
20	0.235	0.213	0.196	0.182	0.169	0.160	0.156	0.189	1.029
30	0.179	0.167	0.154	0.141	0.131	0.122	0.119	0.152	0.222
40	0.143	0.130	0.119	0.109	0.100	0.093	0.095	0.145	0.217
50	0.114	0.102	0.093	0.084	0.077	0.071	0.092	0.144	0.217
60	0.087	0.080	0.072	0.065	0.059	0.056	0.092	0.145	0.222
70	0.068	0.063	0.058	0.053	0.059	0.071	0.095	0.152	1.029
80	0.057	0.053	0.058	0.065	0.077	0.093	0.119	0.189	19.426
90	0.057	0.063	0.072	0.084	0.100	0.122	0.156	1.179	–

values of σ that produce better results. Therefore, it is clear that LFA can aid in identifying the optimal values of both σ and ν.

5 Computational cost

The convergence factors presented in the previous sections alone are not enough to determine the most efficient multigrid method. To make this assessment, we consider the computational cost, which is typically measured by the number of arithmetic operations.

To compare the computational costs associated with the $2h$-, $4h$- and $8h$-coarsening strategies numerically, we analyze the following problem

$$-\Delta u(\mathbf{x}) = f(\mathbf{x}),\ \mathbf{x} \in \Omega,\ u(\mathbf{x}) = g(\mathbf{x}),\ \mathbf{x} \in \partial\Omega, \tag{13}$$

where f and g are chosen such that the exact solution is given by $u(x, y) = sin(\pi x)sin(\pi y)$.

We consider the three triangular domains studied in the previous section: an equilateral triangle ($\alpha = \beta = 60°$), an isosceles right triangle ($\alpha = \beta = 45°$), and an isosceles triangle ($\alpha = \beta = 80°$). For this case, we use the ILU_σ smoother with $\sigma_{2h} = 0.5$, $\sigma_{4h} = -0.1$, and $\sigma_{8h} = -0.5$ (the subscript indicates the coarsening strategy), based on the LFA results obtained in the previous sections.

To perform the numerical experiments, we set the initial residual as $r(0) = 1$ and defined the stopping criterion based on the non-dimensional residual $r(\text{Iter})$, requiring it to be less than 10^{-8}. We considered 11 refinement levels for $2h$-coarsening (the finest mesh has $N_{11} = 525\,825$ nodes), 6 refinement levels for $4h$-coarsening (the finest mesh has $N_6 = 525\,825$ nodes), and 4 refinement levels for $8h$-coarsening (the finest mesh has $N_4 = 131\,841$ nodes).

To measure the performance of the multigrid methods, we counted the number of floating-point operations (flops) during the iterative process, as the choice of hardware did not interfere with the results. For simplicity, we treated additions, multiplications, and divisions as a single Flop. The numerical results are presented in Tables 7, 8 and 9 for the equilateral, right, and isosceles triangles, respectively. These tables show the number of floating-point operations divided by the number of points in the finest grid. Additionally, the values of σ chosen in the previous sections for each coarsening level are applied. The most efficient multigrid smoothers for each strategy are highlighted in bold.

Table 7 Presents the results for the equilateral triangle, showing the type of cycle used and the number of floating-point operations (flops) divided by the number of points in the finest grid

ν	$2h$-coarsening		$4h$-coarsening		$8h$-coarsening	
	Iter.	Flops/N_{11}	Iter.	Flops/N_6	Iter.	Flops/N_4
$F(1,0)$	15	385.53	22	537.55	39	905.29
$F(1,1)$	9	**363.22**	13	**498.09**	22	800.61
$F(2,1)$	8	425.50	10	516.94	14	**699.12**
$F(2,2)$	7	463.78	9	579.22	12	751.75

The experiments use the $\text{ILU}_{0.5}$ smoother for 2 h-coarsening, the $\text{ILU}_{-0.1}$ smoother for 4 h-coarsening, and the $\text{ILU}_{-0.5}$ smoother for 8 h-coarsening

Table 8 Presents the results for the right triangle, showing the type of cycle used and the number of floating-point operations (flops) divided by the number of points in the finest grid

ν	$2h$-coarsening		$4h$-coarsening		$8h$-coarsening	
	Iter.	Flops/N_{11}	Iter.	Flops/N_6	Iter.	Flops/N_4
$F(1,0)$	13	342.09	18	450.68	31	731.79
$F(1,1)$	8	**329.50**	11	**430.65**	17	632.18
$F(2,1)$	7	379.78	10	516.94	12	**607.75**
$F(2,2)$	7	463.78	9	579.22	11	694.06

The experiments use the $\text{ILU}_{0.5}$ smoother for 2 h-coarsening, the $\text{ILU}_{-0.1}$ smoother for 4 h-coarsening, and the $\text{ILU}_{-0.5}$ smoother for 8 h-coarsening

Table 9 Presents the results for the isosceles triangle, displaying the type of cycle used and the number of floating-point operations (flops) divided by the number of points in the finest grid

ν	$2h$-coarsening		$4h$-coarsening		$8h$-coarsening	
	Iter.	Flops/N_{11}	Iter.	Flops/N_6	Iter.	Flops/N_4
$F(1,0)$	16	**407.24**	42	971.92	90	2011.30
$F(1,1)$	11	430.65	22	801.55	46	1609.09
$F(2,1)$	9	471.22	15	**745.53**	30	1430.11
$F(2,2)$	9	579.22	13	810.09	23	1386.30
$F(3,2)$	–	–	–	–	19	1383.55
$F(3,3)$	–	–	–	–	16	**1366.50**

The $\text{ILU}_{0.5}$ smoother is used for 2 h-coarsening, the $\text{ILU}_{-0.1}$ smoother for 4 h-coarsening, and the $\text{ILU}_{-0.5}$ smoother for 8 h-coarsening

Note that the best multigrid methods for the equilateral triangle correspond to the $F(1,1)-$cycle for $2h$-coarsening, the $F(1,1)-$cycle for $4h$-coarsening, and the $F(2,1)-$cycle for $8h$-coarsening. For the right isosceles triangle, the optimal methods are the $F(1,1)-$cycle for both $2h$- and $4h$-coarsening, and the $F(2,1)-$cycle for $8h$-coarsening. For the isosceles triangle, the best methods are the $F(1,0)-$cycle for $2h$-coarsening, the $F(2,1)-$cycle for $4h$-coarsening, and the $F(3,3)-$cycle for $8h$-coarsening.

Based on the results, $8h$-coarsening incurs a significantly higher computational cost compared to both $2h$- and $4h$-coarsening. However, the computational costs for $2h$- and $4h$-coarsening are similar, making both viable options for real-world applications. Among these, $4h$-coarsening presents notable advantages.

Firstly, $4h$-coarsening requires less memory. For instance, after 11 refinement levels, $2h$-coarsening uses 702,132 nodes, while $4h$-coarsening reaches the same refinement level with just 6 refinement levels and only 561,291 nodes about 20% less computational storage.

Additionally, in parallel computing, $4h$-coarsening offers a practical benefit by reducing data exchange. Fewer refinement levels mean fewer coarse grids to process, which decreases the need for data transfer between processors, thus improving computational efficiency.

6 Conclusion

We have presented robust and efficient geometric multigrid methods for hierarchical triangular grids, utilizing standard ($2h$) and aggressive ($4h$ and $8h$) coarsening strategies. Through local Fourier analysis (LFA) applied to triangular grids for the Poisson problem, we studied the theoretical convergence of the multigrid methods. The concepts of low and high frequencies, as well as harmonic spaces, were adapted to accommodate the aggressive coarsening strategies.

Considering both the convergence factor and computational cost, we found that $4h$-coarsening is as robust and efficient as $2h$-coarsening. Moreover, it offers significant advantages for parallel computing, particularly with lower memory storage requirements. These findings confirm that the ILU smoother adaptation for triangular grids proposed in this work is highly effective.

Acknowledgements The authors would like to acknowledge the Graduate Program in Numerical Methods for Engineering (PPGMNE) of the Federal University of Parana (UFPR). The work of Grazielli Vassoler Rutz is supported by the Federal Institute of Education, Science and Technology of Santa Catarina (IFSC).

Declarations

Conflict of interest The authors declare that there are no Conflict of interest related to this study.

References

Axelsson O (1994) Iterative solution methods. Cambridge University Press, New York

Brannick J, Hu X, Rodrigo C, Zikatanov L (2015) Local Fourier analysis of multigrid methods with polynomial smoothers and aggressive coarsening. Numer Math Theory Methods Appl 8(1):1–21

Buleev NI (1960) A numerical method for the solution of two-dimensional and three-dimensional equations of diffusion. Math Sb 51:227–238

Chan TF (1991) Fourier analysis of relaxed incomplete factorization preconditioners. SIAM J Sci Stat Comput 12(3):668–680

Gaspar FJ, Gracia JL, Lisbona FJ (2009) Fourier analysis for multigrid methods on triangular grids. SIAM J Sci Comput 31(3):2081–2102

Gaspar FJ, Gracia JL, Lisbona FJ, Rodrigo C (2009) On geometric multigrid methods for triangular grids using three-coarsening strategy. Appl Numer Math 59(7):1693–1708

Hackbusch W (1994) Iterative solution of large sparse linear systems of equations. Applied mathematical sciences series, no. 95. Springer

Hackbusch W (1985) Multi-grid methods and applications. Springer, Berlin

Johannsen K (2005) A robust 9-point ILU smoother for anisotropic problems. IWR preprint

Khalil M (1989) Local mode smoothing analysis of various incomplete factorization iterative methods. In: Robust multi-grid methods. Springer, pp 155–164

Oertel K-D, Stüben K (1989) Multigrid with ILU-smoothing: systematic tests and improvements. In: Robust multi-grid methods. Springer, pp 188–199

Oliphant TA (1961) An implicit numerical method for solving two-dimensional time-dependent diffusion problems. Q Appl Math 19:221–229

Oliphant TA (1962) An extrapolation process for solving linear systems. Q Appl Math 20:257–267
Oliveira ML, Pinto MAV, Gonçalves SFT, Rutz GV (2018) On the robustness of the XY-Zebra-Gauss-Seidel smoother on an anisotropic diffusion problem. Comput Model Eng Sci 117(2):251–270
Pinto M, Rodrigo C, Gaspar F, Oosterlee C (2016) On the robustness of ILU smoothers on triangular grids. Appl Numer Math 106:37–52
Rodrigo C, Gaspar FJ, Lisbona FJ (2012) Geometric multigrid methods on triangular grids: application to semi-structured meshes. Lambert Academic Publishing, Saarbrücken
Rutz GV, Pinto MAV, Gonçalves SFT (2019) On the robustness of the multigrid method combining ILU and partial weight applied in an orthotropic diffusion problem. Revista Internacional de Métodos Numéricos para Cálculo y Diseño en Ingeniería 35(1)
Silva LP, Rutyna BB, Santos Righi AR, Villela Pinto MA (2021) High order of accuracy for Poisson equation obtained by grouping of repeated Richardson extrapolation with fourth order schemes. Comput Model Eng Sci 128(2):699–715
Stevenson R (1994) Robust multi-grid with 7-point ILU smoothing. In: Multigrid methods IV. Springer, pp 295–307
Stevenson R (1994) Modified ILU as a smoother. Numer Math 68(2):295–309
Stüben K, Trottenberg U (1982) Multigrid methods: fundamental algorithms, model problem analysis and applications. In: Multigrid methods. Springer, pp 1–176
Trottenberg U, Oosterlee CW, Schüller A (2001) Multigrid. Academic Press, New York
Varga RS (1960) Factorization and normalized iterative methods. In: Langer RE (ed) Boundary problems in differential equations. University of Wisconsin Press, Madison, pp 121–142
Varga RS (1962) Matrix iterative analysis. Prentice-Hall Inc., Englewood Cliffs
Wesseling P (1982) Theoretical and practical aspects of a multigrid method. SIAM J Sci Stat Comput 3(4):387–407
Wesseling P (1992) An introduction to multigrid methods. Wiley, Chichester
Wesseling P, Sonneveld P (1980) Numerical experiments with a multiple grid and a preconditioned Lanczos type method. In: Approximation methods for Navier–Stokes problems. Springer, pp 543–562
Wienands R, Joppich W (2005) Practical Fourier analysis for multigrid methods. Chapman and Hall/CRC Press
Wittum G (1989) Linear iterations as smoothers in multigrid methods: theory with applications to incomplete decompositions. IMPACT Comput Sci Eng 1(2):180–215
Wittum G (1989) On the robustness of ILU smoothing. SIAM J Sci Stat Comput 10(4):699–717
Zubair HB, Oosterlee CW, Wienands R (2007) Multigrid for high-dimensional elliptic partial differential equations on non-equidistant grids. SIAM J Sci Comput 29(4):1613–1636